

In the laboratory, the design benefits have been observed by setting up the system in Fig. 1. The mirror was formed by immersing the cleaved fibre endface in a drop of mercury. Full modulation depth, 100% of the Y power amplitude, was always observed for all Φ angles. The Φ angles of 0° , 90° and multiples, provided no output Y beam, as expected.

Conclusion: It has been shown that the single-ended birefringent fibre optic sensor has several advantages over its double-ended counterpart. In particular, the lack of a DC offset and a doubling of the sensor sensitivity are features worth exploiting. The single-ended system is no longer dependent on polariser/fibre angle since full modulation is always observed. Once a Y output beam has been obtained, the amplitude of the power will generate a 100% modulation depth in the sensor response. The design presented here can be used to enhance present sensor configurations as well as simplify applications involving embedded optical fibres. These design considerations are now being examined in our laboratory for including in smart sensor structures.

21st September 1992

R. C. Gauthier (Dept. of Physics & Astronomy, Laurentian University, Sudbury, Ontario, Canada P3E 2C6)

References

- 1 BOCK, W. J., DOMANSKI, A. W., and WOLINSKI, T. R.: 'Influence of high hydrostatic pressure on beat length in highly birefringent single-mode bow tie fibres', *Appl. Opt.*, 1990, **29**, (24), pp. 3484-3488
- 2 GAUTHIER, R. C.: 'External birefringent fibre optic heart rate monitor', *Optics & Laser Technol.*, 1992, **16**, (7) (accepted for publication)
- 3 GAUTHIER, R. C., and DHLIWAYO, J.: 'Birefringent fibre-optic pressure sensor', *Optics and Laser Technology*, 1992, **25**, (3) (accepted for publication)

POWER AND EFFICIENCY LIMITS IN SINGLE-MIRROR LIGHT EMITTING DIODES WITH ENHANCED INTENSITY

N. E. J. Hunt, E. F. Schubert, D. L. Sivco, A. Y. Cho and G. J. Zydzik

Indexing term: Light emitting diodes

The principle of enhanced emission intensity in a single-mirror light emitting diode (LED) is demonstrated by placing an InGaAs multi-quantum-well active region in the antinode of the optical mode created by a nearby metallic mirror, thus enhancing emission along the optical axis by up to four times. Multiple-well LED structures exhibit enhanced efficiencies similar to that of a perfect isotropic emitter. The emission intensity of single-well LEDs is limited by band filling.

Light emitting diodes (LEDs) are preferable to lasers for short distance fibre communications because of their greater reliability and lower cost, although the optical power coupled into a fibre is smaller. Because their emission is purely spontaneous, LEDs are less susceptible to power changes with temperature. Therefore, it is of interest to seek improvements in output intensity without resorting to a structure with optical gain. By positioning an optical reflector behind a thick spontaneously emitting surface, the far field intensity is doubled compared to an LED without a mirror [1]. However, if the active region is thin, and it is placed in the antinode of the optical mode, the normal incidence emission can be enhanced by a factor of four. Deppe *et al.* [2] demonstrated with a single quantum well structure that the enhancement and inhi-

tion of emission depends on the quantum-well placement. However, the emission intensity of such single-mirror devices has not been investigated quantitatively. We have fabricated single- and multi-quantum-well LEDs in order to determine the power, efficiency, and spectral characteristics of such devices.

Fig. 1 shows the schematic structure for a single-quantum-well LED. The current is injected from a $10\ \mu\text{m}$ diameter silver

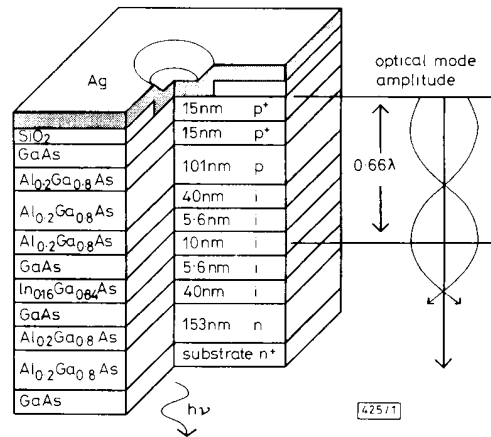


Fig. 1 Device structure for single-quantum-well LED optically coupled to silver mirror

Multiple well structures were also grown; the contact circle is $10\ \mu\text{m}$ in diameter

cap which simultaneously acts as a 96% reflector. The amplitude of the normal incidence optical mode is also shown with the active quantum well in the antinode. The enhancement process can also be explained by constructive interference of the direct and reflected beams in the normal direction, giving a formula of $(1 + R^{1/2})^2$ for the maximum enhancement. For a reflectance $R = 0.96$, ignoring substrate-to-air reflections, the antinode placement enhances the normal emission intensity through the substrate by a factor of 3.85. Because the metal mirror is in close proximity to the quantum well, the antinode position changes slowly with wavelength, ensuring that the enhancement is mostly preserved over the entire spectral range of the LED.

One, four, six, and eight well structures were grown by molecular beam epitaxy with the same 10 nm thick $\text{In}_{0.16}\text{Ga}_{0.84}\text{As}$ wells, and with 5.6 nm thick GaAs barriers. The confining layers are made thinner than in the single-quantum-well sample in order to centre the active region in the optical antinode. As more wells are added, they cannot all be positioned exactly in the antinode, reducing the theoretical intensity enhancement achievable with the single-mirror structure. For one, four, six, and eight quantum wells the theoretical enhancements are 3.8, 3.4, 2.8, and 2.2, respectively. For the eight-well structure the active region is approaching a thickness of $\lambda/2$ whereby the maximum enhancement is 2.0. The enhancement for greater thicknesses than this is just under or over 2, depending on positioning.

The maximum usable current at which an LED can operate is determined by a number of factors, including the effects of band filling. Fig. 2 shows the emission spectra from the top of a single-quantum-well device with a thin 30 nm semitransparent top silver mirror. The emission is narrow at an injection current of 0.6 mA, but begins to broaden by 2 mA and is very broad by 6 mA. This indicates very high carrier concentrations, and the broad spectra would result in a large amount of chromatic dispersion in an optical fibre. Clearly a single quantum well cannot be pumped very hard and therefore cannot achieve high spontaneous output intensities. It can be calculated from rate equations that for a reasonable carrier lifetime of 1 ns, a 1 mA pump current into a single well at a current density of $1.3\ \text{kA}/\text{cm}^2$ results in a carrier density of

$8 \times 10^{12} \text{ cm}^{-2}$ or $\sim 8 \times 10^{18} \text{ cm}^{-3}$. We therefore expect that band filling occurs at such injection currents.

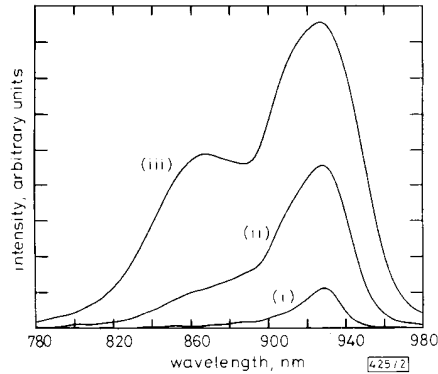


Fig. 2 295 K spectra through top of single-quantum-well device with 30 nm thick semitransparent silver top mirror

The spectra at three different pump currents clearly show the effects of band filling

- (i) 0.6 mA
- (ii) 2.0 mA
- (iii) 6.0 mA

The light output from the substrate against current was measured for the devices, and the results are shown in Fig. 3 at normal incidence. The spectrally integrated intensity is

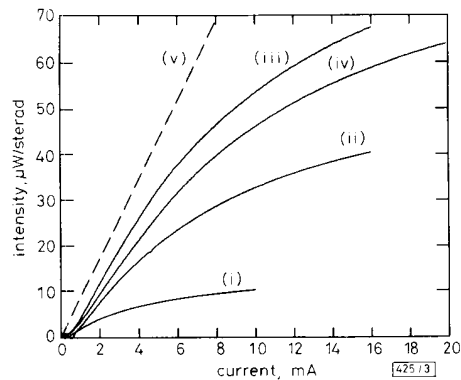


Fig. 3 Intensity in narrow solid angle normal to emitting substrate surface against pump current

Curves for 1, 4, 6, and 8 quantum-well samples are shown, as is the line representing a perfect efficiency, isotropically emitting active region without mirror

- (i) One quantum well
- (ii) Four quantum wells
- (iii) Six quantum wells
- (iv) Eight quantum wells
- (v) Perfect isotropic emitter

measured with a calibrated small area detector placed 7.5 cm away from the devices. Subsequently the intensity per steradian is calculated. Although the intensity drops with angle from the normal, the normal incidence value is most important because even by using lenses only a small solid angle of the LED emission is coupled into a fibre. The dashed line on the graph corresponds to the calculated light intensity for a 100% internal quantum efficiency isotropic emitter with an ideal $R = 0$ antireflection coating. This efficiency cannot be achieved in conventional LEDs with a nonunity internal quantum efficiency. Our devices approach this efficiency, even without the use of antireflection coatings. The initial kink in the curves is caused by a small leakage current of 300–600 μA .

The one-quantum-well sample has a lower initial efficiency than the other samples, probably because of reduced capture of the carriers in the quantum well. It is clear, however, that its light output saturates at a low output current. This saturation is caused partly by the combination of band filling and the effect of the GaAs substrate absorption of light with shorter wavelengths than 890 nm. With the degree of band filling seen in Fig. 2, however, it is clear that the single quantum well cannot be pumped at high currents. The light against current curves for the multiquantum-well samples exhibit less current saturation and achieve intensity levels that are useful for communications. How much light is coupled into a fibre depends on the geometry of the coupling optics and the thickness of the substrate. Larger diameter devices would give similar low-current efficiencies, and neglecting heating can achieve higher final powers, although with proportionally higher current. The initial efficiencies are similar to that of a perfect isotropic emitter, or 8.7 $\mu\text{W/sterad/mA}$ in air at normal incidence from a material with refractive index $n = 3.5$ at a wavelength $\lambda_0 = 0.93 \mu\text{m}$. This efficiency is given by $(1240/\lambda_0)(1/(4\pi n^2))$. Considering the theoretical enhancement factors of up to 4, it is possible for future devices to perform even better. We do not expect the optical coupling with the mirror to significantly affect device speed, as we calculate [3] that the Einstein spontaneous emission factor A_{sp} will be increased by less than 5%.

Fig. 4 shows the top emission spectra through the silver for all four growths at an injection current of 2.0 mA per well.

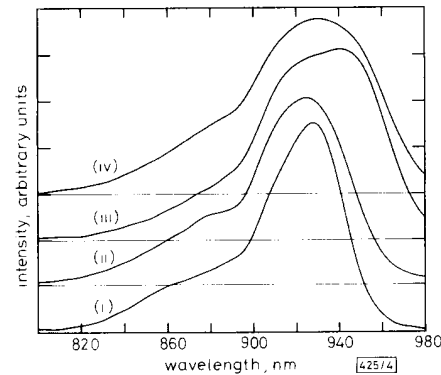


Fig. 4 Spectra through top of semitransparent silver mirror for 1, 4, 6, and 8 quantum well samples for 2, 8, 12, and 16 mA pump currents, respectively

Because this corresponds to equal currents per well, the band filling is similar for the four spectra

- (i) One quantum well
- (ii) Four quantum wells
- (iii) Six quantum wells
- (iv) Eight quantum wells

This should result in similar carrier densities in the wells and therefore similar spectra. Although the growths are not identical, it is clear from the curves, and by comparison with Fig. 2, that the carrier densities must indeed be similar. Again this shows that more wells are advantageous to achieving high output powers. The band filling associated with high carrier densities results in higher chromatic dispersion in optical fibres, limiting communications bandwidth and distance. Band filling can also be a major limitation to the power achievable in resonant cavity light emitting diodes (RCLEDs) [4], where the active region is placed in the optical antinode of the resonance between two mirrors.

In conclusion, we have demonstrated for the first time that intensities approaching that of a perfect isotropic emitter can be obtained in a multiquantum-well single-mirror LED. By placing the active region in the antinode of the optical mode, an intensity enhancement of up to four times can be obtained. The highest efficiency was observed from a six-quantum-well sample, which has a theoretical enhancement of 2.8 at this wavelength. We have shown that whereas the single-quantum-well LED structure cannot operate at high intensities due to

band filling, single-mirror multiquantum-well LEDs exhibit high efficiencies at current densities useful for optical fibre communications.

21st September 1992

N. E. J. Hunt, E. F. Schubert, D. L. Sivco, A. Y. Cho and G. J. Zydzik (AT&T Bell Laboratories, Murray Hill, NJ 07974, USA)

References

- 1 KATO, T., SUSAWA, H., HIROTANI, M., SAKA, T., OHASHI, Y., SHICHI, E., and SHIBATA, S.: 'GaAs/GaAlAs surface emitting IR LED with Bragg reflector grown by MOCVD', *J. Cryst. Growth*, 1991, **107**, pp. 832-835
- 2 DEPPE, D. G., CAMPBELL, J. C., KUCHIBHOTLA, R., ROGERS, T. J., and STREETMAN, B. G.: 'Optically-coupled mirror-quantum well InGaAs-GaAs light emitting diode', *Electron. Lett.*, 1990, **27**, pp. 1165-1166
- 3 UJIHARA, K.: 'Spontaneous emission and the concept of effective area in a very short optical cavity with plane-parallel dielectric mirrors', *Jpn. J. Appl. Phys.*, 1991, **30**, pp. L901-L903
- 4 SCHUBERT, E. F., WANG, Y.-H., CHO, A. Y., TU, L.-W., and ZYDZIK, G. J.: 'Resonant cavity light emitting diode', *Appl. Phys. Lett.*, 1992, **60**, pp. 921-923

0.98 μm STRAINED-LAYER GaInAs/GaInAsP/GaInP QUANTUM WELL LASERS

G. Zhang, J. Näppi, A. Ovtchinnikov, P. Savolainen and H. Asonen

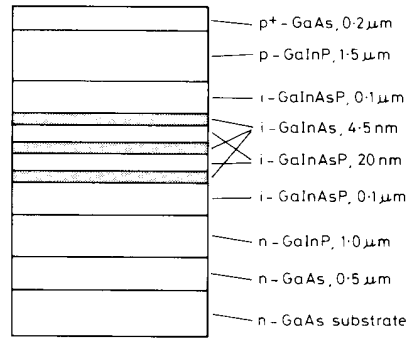
Indexing terms: Semiconductor lasers, Lasers

Strained-layer GaInAs/GaInAsP/GaInP separate-confinement-heterostructure multiquantum well lasers which emit at a wavelength of 0.98 μm are reported. These lasers exhibit a low threshold current density of 153 A/cm² and high characteristic temperature up to 235 K. The internal waveguide loss and internal quantum efficiency are 5.0 cm⁻¹ and 83%, respectively. Singlemode continuous wave operation is found up to an output power of 80 mW at room temperature for an HR/AR coated 5.5 \times 800 μm^2 ridge waveguide laser. waveguide laser.

Recently, aluminium-free strained-layer GaInAs/GaAs/GaInP separate-confinement-heterostructure quantum well (SCH-QW) lasers have become of great interest [1-5] because of their superior resistance over AlGaAs lasers to rapid degradation by dark line defect catastrophic growth and facet oxidation [1, 6]. Moreover, the aluminum-free laser structure is more suitable for diode fabrication by selective chemical etching and epitaxial regrowth [5]. However, we observed that the carrier population in the confinement GaAs layers was significant for this type of laser, when emitting at $\lambda \leq 0.98 \mu\text{m}$. This high carrier population, i.e. poor carrier confinement, resulted in a low characteristic temperature T_0 and small external differential quantum efficiency η_d . We expect that the carrier confinement can be improved if the GaAs confinement layers can be replaced by higher energy bandgap layers. In this Letter, we report a strained-layer GaInAs/GaInAsP/GaInP SCH-QW laser, emitting at 0.98 μm , in which the confinement layers are Ga_{0.8}In_{0.2}As_{0.62}P_{0.38} (abbreviated as GaInAsP), lattice matched to GaAs, with an energy bandgap of $E_g = 1.60 \text{ eV}$.

The strained-layer GaInAs/GaInAsP/GaInP SCH-QW laser structure, grown by gas-source molecular beam epitaxy, is shown in Fig. 1. The active region comprises three 4.5 nm thick Ga_{0.8}In_{0.2}As quantum wells (later abbreviated as GaInAs). The cladding layers are Ga_{0.51}In_{0.49}P (abbreviated as GaInP). The doping levels of the n-type and p-type GaInP cladding layers are 1.0×10^{18} and $8.0 \times 10^{17} \text{ cm}^{-3}$, respec-

tively. The p⁺-GaAs contact layer is highly doped, $3.0 \times 10^{19} \text{ cm}^{-3}$, to minimise contact resistance.

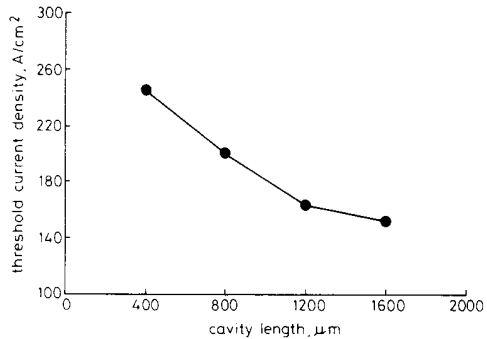


[474/1]

Fig. 1 Schematic structure of strained-layer GaInAs/GaInAsP/GaInP separate-confinement-heterostructure laser consisting of three quantum wells

Broad-area Fabry-Perot cavity lasers and ridge-waveguide lasers with cavity length L between 400 and 1600 μm were processed by standard methods. The lasers, soldered on submounts, were tested under pulse and CW mode operations at temperatures between 10 and 70°C.

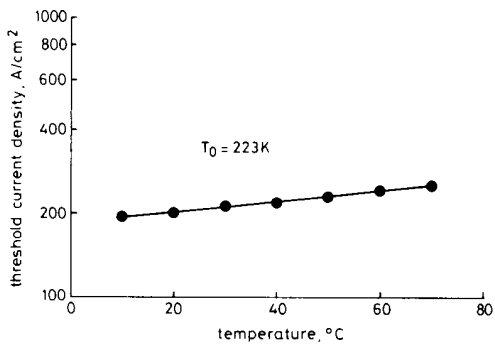
As shown in Fig. 2, the threshold current density for the uncoated broad-area lasers ranged from 153 to 245 A/cm², as



[474/2]

Fig. 2 Threshold current density against cavity length for uncoated broad-area laser

L decreased from 1600 to 400 μm . This J_{th} is comparable to the best values of J_{th} reported for GaInAs/GaAs/AlGaAs and GaInAs/GaAs/GaInP lasers [4, 7]. Fig. 3 shows J_{th} against operating temperature for an 800 μm long broad-area laser,



[474/3]

Fig. 3 Threshold current density of 800 μm long broad-area laser run in pulse mode as function of operation temperature